Exchange bias in Fe/Fe_3O_4 core-shell magnetic nanoparticles mediated by frozen interfacial spins

Quy Khac Ong and Alexander Wei
Department of Chemistry, Purdue University, 560 Oval Drive, West Lafayette, Indiana 47907-2084, USA

Xiao-Min Lin
Center for Nanoscale Materials, Argonne National Laboratory, Argonne, Illinois 60439-4803, USA
(Received 21 May 2009; revised manuscript received 14 September 2009; published 23 October 2009)

The magnetization curves of monodisperse Fe/Fe_3O_4 core-shell and Fe_3O_4 hollow-shell nanoparticles reveal an unusual exchange-bias effect. Hysteresis measurements of core-shell particles at 5 K after field cooling exhibit a large loop shift associated with unidirectional anisotropy whereas Fe_3O_4 hollow-shell nanoparticles support much smaller shifts. Both core-shell and hollow-shell particles exhibit sharp demagnetization jumps at low fields associated with a sudden switching of shell moments. Temperature-dependent magnetization of core-shell particles at high fields shows a deviation between field-cooled and zero-field-cooled curves below 30 K, suggesting the presence of frozen spins at the interface. These frozen interfacial spins play an important role in mediating the exchange coupling between the ferromagnetic core and ferrimagnetic shell.

DOI: 10.1103/PhysRevB.80.134418 PACS number(s): 75.75.+a, 61.46.Hk, 75.50.Tt, 75.60.Jk

I. INTRODUCTION

The exchange-bias (EB) effect is manifest by the shifting and broadening of a magnetic hysteresis loop of a sample cooled under an applied field.[1–3] Although the macroscopic model of EB has been in existence for nearly five decades, the microscopic origin of this unique phenomenon is still being actively investigated[4–6] largely because the structural differences at nanometer and even atomic level have a strong impact on exchange coupling.[3,7] EB is typically attributed to the unidirectional coupling between ferromagnetic (FM) and antiferromagnetic (AFM) layers but can also exist in samples having a ferrimagnetic domain,[8] spin glasses,[9] or disordered surface spins.[10,11]

Although the EB effect was first discovered in colloidal magnetic nanoparticle systems,[1] subsequent research has mainly focused on bilayer and multilayer thin films. This is largely because the spin distribution in a three-dimensional core-shell particle is intrinsically more complex than the case of thin films. Furthermore, the size polydispersity and the tendency of particles to aggregate in solution also make quantitative measurements more difficult.[12] However, recent developments in chemical synthesis enable us to create highly uniform core-shell and hollow-shell magnetic nanoparticles with well-defined oxide layers.[13,14] EB has also been proposed as a possible way to overcome the superparamagnetic behavior that limits the application of nanoparticles in magnetic storage media.[15] These developments have rekindled interests to further study exchange-bias behavior in core-shell nanoparticles.[16–21]

Many of the microscopic mechanisms that support exchange bias and related phenomena have yet to be resolved. For example, in many cases the disappearance of EB with increasing temperature does not coincide with the magnetic-ordering temperature (e.g., Néel temperature of AFM layer).[17,22] Recent studies by Ohldag *et al.* using x-ray magnetic circular dichroism revealed uncompensated spins at the FM/AFM bilayer interface, which suggests these "pinned" moments could be responsible for the EB effect.[23] This model has subsequently been adopted to explain EB in several other systems.[12,24] However, others have argued that the domain walls in the AFM layer can be stabilized by either surface roughness[6] or volume defects,[4] which provide a net magnetic moment that enables coupling with the FM domain through exchange interactions. Here, we present a detailed study on the magnetic properties of isolated Fe/Fe_3O_4 core-shell and Fe_3O_4 hollow-shell nanoparticles. By comparing magnetic hysteresis under both field-cooled (FC) and zero-field-cooled (ZFC) conditions at different temperatures and cooling fields, we demonstrate that the exchange anisotropy is indeed mediated by frozen interfacial spins between core and shell domains. Furthermore, we observed a low-field switching behavior in both core-shell and hollow-shell particles, which we attribute to the depinning of ferrimagnetic shell moments.

II. SAMPLE PREPARATION AND STRUCTURE CHARACTERIZATIONS

The monodisperse core-shell and hollow-shell nanoparticles were prepared following procedures by Sun and co-workers.[14] Briefly, Fe nanoparticles were synthesized by the thermal decomposition of $Fe(CO)_5$ at 180 °C in the presence of oleylamine. Subsequent treatment with $(CH_3)_3NO$ for 20 min at 240 °C yielded Fe/Fe_3O_4 core-shell nanoparticles, whereas further heating the nanoparticle solution in air for 2 h at 240 °C yielded Fe_3O_4 hollow-shell nanoparticles (Fig. 1). X-ray diffraction and high-resolution transmission electron microscopy (HR-TEM) showed the Fe core is amorphous and oxide shell is polycrystalline. The nanoparticles were precipitated and resuspended in a 10% weight ratio with dimethyldioctadecylammonium bromide (DDAB) in chloroform, then dried into powder and stored under nitrogen. Magnetic measurements were conducted using a Quantum Design 7 T SQUID magnetometer. Hysteresis loops were obtained at 5 K by sweeping the applied field from 10

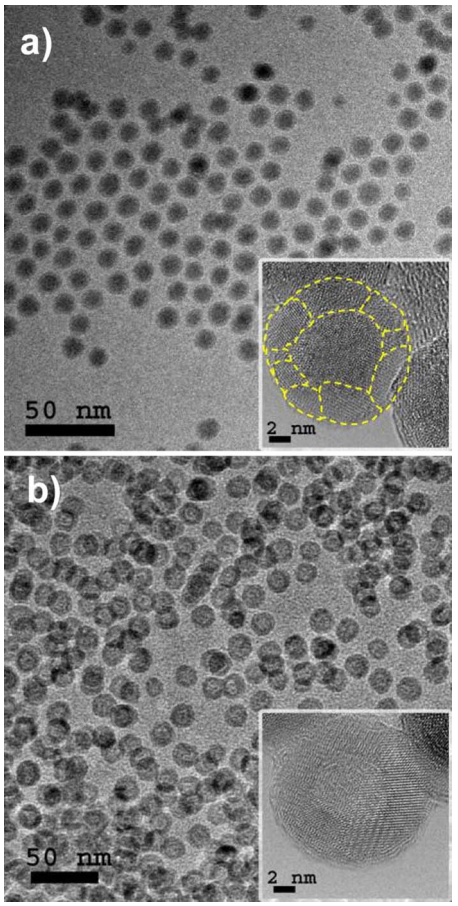

FIG. 1. (Color online) (a) TEM image of Fe/Fe_3O_4 core-shell nanoparticles (13.8 ± 1.0 nm, $N=100$). Inset: HR-TEM image of the core-shell structure with average shell thickness of 2.5 nm. Dashed lines demarcate nanocrystalline domains in the Fe_3O_4 shell. (b) Fe_3O_4 hollow-shell nanoparticles (16.0 ± 1.2 nm, $N=230$) with a shell thickness of 4.5 nm. Inset: HR-TEM image of the hollow-shell nanoparticles.

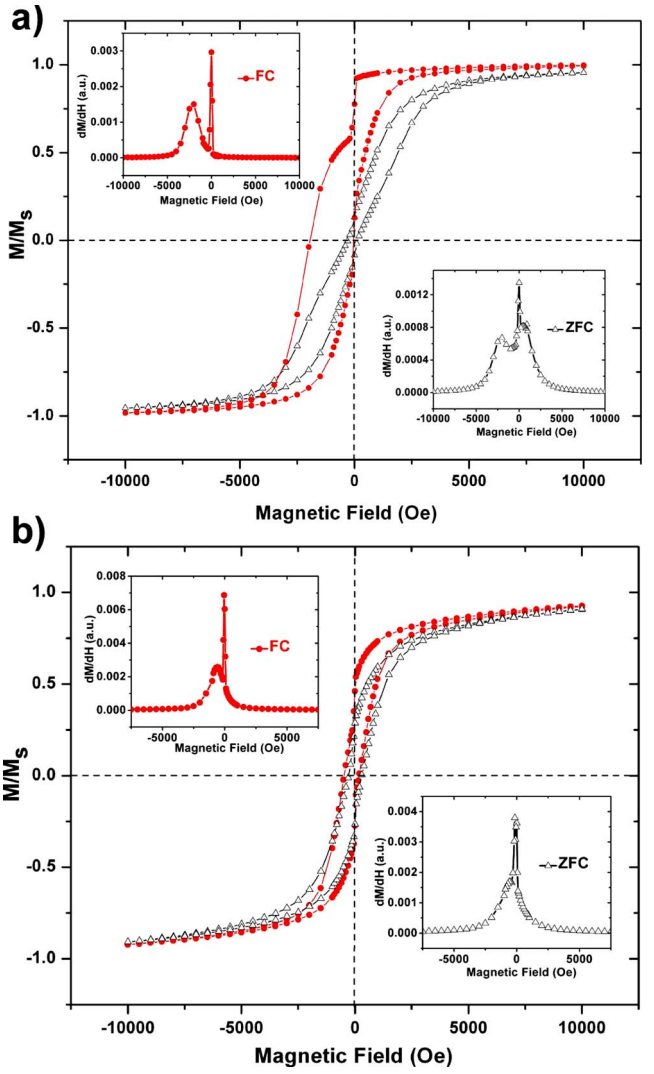

FIG. 2. (Color online) *M-H* hysteresis loops for (a) Fe/Fe_3O_4 core-shell and (b) Fe_3O_4 hollow-shell nanoparticles, under FC (filled circles) and ZFC (open triangles) conditions. Insets: dM/dH plots for core-shell and hollow-shell nanoparticles during the negative sweep direction (from 10 to −10 kOe).

to −10 kOe and back to 10 kOe, after cooling the powder sample under ZFC or a 10 kOe field (FC).

III. MAGNETIC PROPERTIES

Dispersed Fe/Fe_3O_4 core-shell nanoparticles exhibit a large loop shift under FC condition, indicative of strong EB coupling [Fig. 2(a)]. The exchange-bias field, $H_E=1190$ Oe, is similar to an earlier value obtained from 9 nm monodispersed Fe particles exposed to an oxygen gas flow[25] but much larger than that measured for Fe nanoparticles embedded in matrices of iron oxide.[20,26,27] The low values for the latter are presumably due to variations in particle size and oxidation. In comparison, Fe_3O_4 hollow-shell nanoparticles exhibit a much weaker exchange-bias field ($H_E=133$ Oe), showing that the EB effect on the ferrimagnetic shell is quite modest in the absence of the FM core [Fig. 2(b)].

To obtain better insights into the EB coupling observed in the core-shell nanoparticles, we first consider the classic phenomenological Meiklejohn-Bean (MB) model of FM/AFM coupling. The MB model is in fact mostly applicable to layered structures with fully uncompensated antiferromagnetic interfaces[1,3,8] but can still provide some qualitative understanding of our spherical core-shell system. The exchange-bias field predicted by the MB model is given by

$$H_E = n\frac{\Delta\sigma}{M_{\mathrm{FM}}t_{\mathrm{FM}}} = n\frac{2J_{ex}\mathbf{S}_{\mathrm{FM}}\cdot\mathbf{S}_{FI}}{a^2 M_{\mathrm{FM}}t_{\mathrm{FM}}}, \quad (1)$$

where $\Delta\sigma$ is the interfacial exchange-energy density, J_{ex} is the interfacial exchange constant, a is the lattice constant for the ferrimagnetic layer (substituting for the AFM layer), $\mathbf{S}_{i,i=\mathrm{FM}orFI}$ represent individual spin moments in the ferromagnetic and ferrimagnetic layers, respectively, M_{FM} and t_{FM} are the saturation magnetization and effective thickness of the ferromagnetic layer, and n/a^2 is the number of exchange-coupled bonds across the interface per unit area. For a spherical ferromagnetic core with a diameter of D_{FM}, the effective thickness of ferromagnetic layer t_{FM} is $1/6D_{\mathrm{FM}}$.[3]

We use $M_{FM}=1714$ emu/cm^3, $a=0.84$ nm,[28] and $t_{FM} \approx 1.5$ nm in our model calculation. Without the in-depth knowledge of interfacial structure, it is difficult to determine whether the value of the exchange constant J_{ex} is closer to the direct exchange constant in metallic systems [$J_{ex} \approx 10^{-14}$ erg (Ref. 29)] or the superexchange constant in ferrite system [$J_{ex} \approx 2.8 \times 10^{-15}$ erg (Ref. 30)]. The theoretical values of H_E calculated from both values are ~111 kOe (direct exchange) and ~31 kOe (superexchange), respectively, when $n=1$. The experimentally observed H_E value in our system is about 1–4 % of the theoretical prediction, implying $n \ll 1$. This is consistent with our hypothesis below that only a small fraction of interfacial spins control the exchange bias. The exchange anisotropy constant ($K_{EB}=M_{FM}H_E t_{FM}$) at 5 K is about 0.3 erg/cm^2, which is close to the value obtained in the bilayer thin film of Fe/Fe_3O_4.[31,32]

In addition to the large EB-induced loop shift, the hysteresis loop of the core-shell nanoparticles also features an abrupt demagnetization or "jump" at low field (ΔM), evident in both positive- and negative-field sweep directions and under both FC and ZFC conditions. The sudden decrease in magnetic moment is more clearly represented by a sharp peak near zero field when dM/dH is plotted (insets in Fig. 2). When the field sweeps from 10 kOe to 100 Oe under FC the magnetization decreases by just 7%, indicating the majority of the magnetic moments are pinned in the direction of the cooling field. The low-field jump occurs between 100 and −200 Oe, and accounts for 31% of the overall magnetization (M_s). The relative intensity of the low-field jump with ZFC is smaller but still accounts for 7.9% of the total magnetization. Similar but less dramatic low-field jumps are also observed with hollow-shell nanoparticles. They are less easily discerned from the M-H plot due to the narrow hysteresis loop but are clearly resolved in dM/dH plots. The jump accounts for ~20% of the overall magnetization for both FC and ZFC conditions. The fact that the low-field jumps are observed in both core-shell and hollow-shell particles indicates that their origin lies in the ferrimagnetic shell region.

Close examination using HR-TEM reveals that the Fe_3O_4 shells are comprised of randomly oriented nanocrystalline domains with sizes on the order of the thickness of the shell [Fig. 1(a), inset]. This suggests that the low-field jump may be due to a sudden reorientation of moments along their respective easy axes, when the magnetocrystalline anisotropy becomes dominant at low field. A simple estimate of the Zeeman energy for a 2.5 nm Fe_3O_4 crystal at 100 Oe is ~0.2 meV, which is below the thermal energy at 5 K (~0.4 meV) and also the magnetocrystalline anisotropy energy (~0.7 meV) derived from the bulk anisotropy constant.[33]

The narrow-size dispersity and well-defined thickness of the oxide shells allow us to determine the percentage of shell moments ($\Delta M/M_{shell}$) that participate in the low-field jump (Table I). The demagnetizations of both types of particles are in fact comparable under ZFC condition once the magnetic contribution of the Fe core is accounted for, and indicate that a portion of the low-field jump in core-shell particles is independent of the cooling field. However, the low-field jump for core-shell particles under FC condition is nearly four times larger relative to the other cases. We consider this to be a consequence of the pinning of shell moments by the aligned frozen spins at the core-shell interface (see below).

TABLE I. Intensity of the low-field jump (ΔM) relative to total magnetization (M_s) and shell magnetization (M_{shell}).

		$\Delta M/M_s$ (%)	$\Delta M/M_{shell}$ [a] (%)
Core-shell	FC	31	74
	ZFC	7.9	19
Hollow-shell	FC	21	21
	ZFC	17	17

[a]$\Delta M/M_{shell}$ for core-shell particles is obtained based on the bulk saturation values of α-Fe (220 emu/g) and Fe_3O_4 (84 emu/g) (Ref. 20), and a core diameter of 8.8 nm and shell thickness of 2.5 nm.

Discontinuous, step-like transitions have been observed previously in the magnetization switching of thin films[22,34] and also for nanoparticles[12,16] but may exist for different reasons. For example, Leighton *et al.* have shown that a two-stage magnetization reversal can occur in specially prepared AFM bilayers when the applied field bisects the anisotropic axes of twinned AFM domains.[34] In this case, the kink in the hysteresis loop occurs only on one side, where magnetization undergoes a coherent rotation rather than domain nucleation. In our core-shell nanoparticle system, the ferrimagnetic shell domains are randomly oriented and do not meet the criterion of the bilayer model above. In addition, the low-field jump observed for core-shell nanoparticles occurs on both sides of the hysteresis loop. There is, however, some common underlying physics between our system and the bilayer system above: magnetocrystalline anisotropy (in our case, within the shell) may also be contributing toward the low-field switching behavior. Tracy *et al.* also observed a low-field jump in Co/CoO core-shell nanoparticles which they attributed to small ferromagnetic clusters at the metal/oxide interface.[16] Similar low-field jumps have also been reported for Fe_3O_4/CoO bilayer[22] and for Fe/γ-Fe_2O_3 core-shell particles[12] but no further analyses were provided for these cases.

The temperature-dependent magnetization of core-shell nanoparticles provides important insights into the basis for the EB effect. Measurements were obtained under FC and ZFC conditions, using two different cooling and measurement fields [Fig. 3]. At 3 Oe, both FC and ZFC curves peak at 115 K (blocking temperature T_B) followed by a magnetization decay approximating a $1/T$ relation, indicating that the nanoparticles are well dispersed in the DDAB matrix. At 10 kOe, the M-T relationship is dominated by spin-wave excitation with a temperature dependence of $M=M_s(1-bT^{1.9})$ [Fig. 3(b), inset]. The decay exponent of 1.9 deviates from the bulk value of 1.5 but is consistent with theoretical predictions based on the reduced density of states in nanoparticles.[35]

A more striking feature is the notable difference between ZFC and FC curves below 30 K even at very high magnetic field (10 kOe) [Fig. 3(b)]. At 5 K, this difference accounts for 5% of the total magnetization. Even with a much higher cooling field (50 kOe), this difference persists and only de-

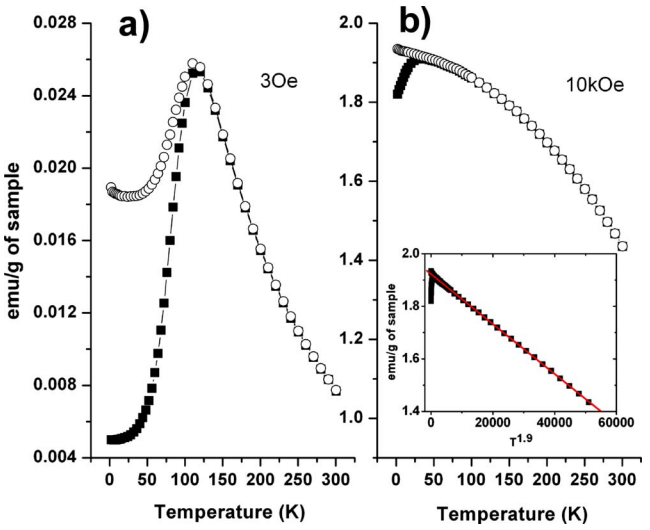

FIG. 3. (Color online) Magnetization vs temperature curves of Fe/Fe_3O_4 core-shell nanoparticles under ZFC (filled squares) and FC (open circles) using cooling and measurement fields of (a) 3 Oe and (b) 10 kOe. Inset in panel (b) shows the data plotted vs $T^{1.9}$.

creases slightly (3.4% at 5 K). We postulate that this difference arises from the incomplete alignment of interfacial spins between FM core and ferrimagnetic shell as well as spins on the outer shell surface under ZFC. Surface spins of ferrimagnetic spinel nanoparticles are known to be disordered, attributed to broken exchange bonds at the surface.[10] These spins are subject to local surface anisotropy and can be trapped at low temperatures. Thus, when the sample is cooled under a 10 kOe field, the surface/interfacial spins will be aligned with the magnetic field. Under ZFC, the surface/interfacial spins are frozen in random directions with a net zero moment and do not respond to measurement fields below 30 K. Above this temperature however, thermal energy can override the local anisotropy and cause surface and especially interfacial spins to align with the external fields. Therefore, the different orientation of the frozen spins at low temperatures leads to the variation in the ZFC and FC magnetization curves in Fig. 3(b). The convergence of these curves above 30 K indicates that the effective local anisotropy is on the order of $k_BT \sim 2.6$ meV ($T=30$ K).

The unidirectional alignment of frozen interfacial spins with FC can explain the strong EB coupling between the

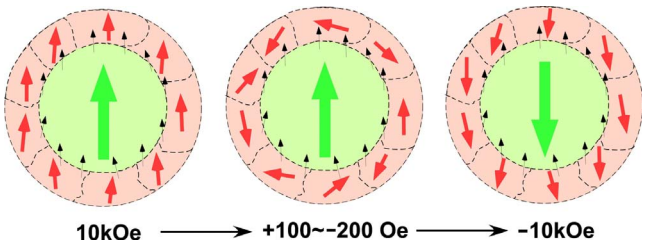

FIG. 4. (Color online) Model of spin orientations in core-shell nanoparticle during hysteresis sweep from 10 to −10 kOe under FC. Ferromagnetic and local ferrimagnetic moments are represented by heavy arrows; frozen interfacial spins are represented by small black arrows.

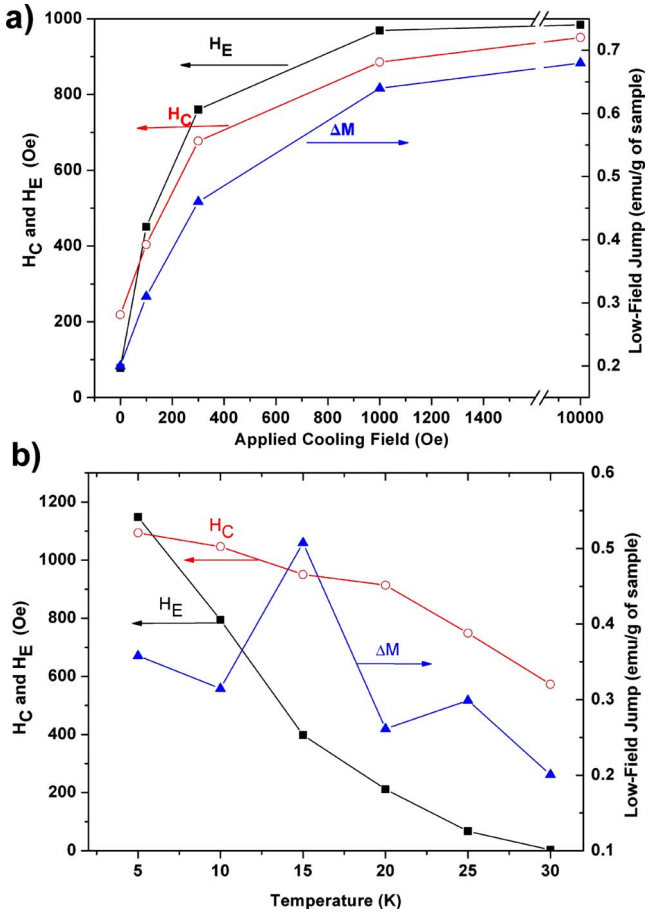

FIG. 5. (Color online) For core-shell particles: (a) exchange-bias field H_E, coercivity H_C, and low-field jump ΔM as a function of applied cooling field; measurements were performed at 5 K. (b) H_E, H_C and ΔM measured after the sample was cooled down to different temperatures under a 10 kOe field (Ref. 36).

core and shell moments. At low temperatures, the interfacial spins are pinned into alignment and provide maximum exchange coupling for directing both the core and shell moments along the field direction, down to 100 Oe [Fig. 4, left]. As the field drops further, the unidirectional anisotropy is superseded by magnetocrystalline anisotropy, resulting in an abrupt demagnetization of the shell [Fig. 4, center]. Under ZFC, the interfacial spins are frozen into random directions, which reduces the exchange coupling between the core and the shell. Consequently, the contribution of shell moments to the low-field jump is much lower (19%, Table I) because a fraction of these moments are pinned along the magnetic field direction at the onset of the jump. A similarly modest EB effect can also be seen in the hollow-shell nanoparticles, presumably mediated by the net alignment of pinned surface spins or interfacial spins with the ferrimagnetic domains. However, this effect is relatively small without the FM core.

Further evidence supporting the role of frozen interfacial spins in EB can be found by examining the dependency of coercivity (H_C) and H_E on cooling field and temperature. The data was obtained by maintaining the core-shell nanoparticles at 300 K for 10 min at zero field, then cooling to 5 K at a rate of −10 K/min under various field strengths [Fig.

5(a)], or by cooling particles to selected temperatures under a 10 kOe field [Fig. 5(b)]. Both H_C and H_E increase with cooling field due to a larger number of interfacial spins frozen in the field direction and a subsequent increase in exchange coupling. The low-field jump ΔM shows a similar trend as it is also affected by the percentage of interfacial spins frozen in the field direction. The dependency on cooling field diminishes above 1 kOe as the number of aligned interfacial spins reaches saturation. On the other hand, H_E decreases with rising temperature and approaches zero at 30 K, above which the interfacial spins are prone to rotate under thermal excitation and can no longer provide an EB field. However, coercivity H_C does not decrease to zero and its value approaches the intrinsic H_C of a core-shell particle without exchange bias. Interestingly, ΔM does not show a clear monotonic dependence on temperature. A repeated measurement under identical conditions confirms the observed fluctuation in ΔM with increasing temperature (data not shown). One possibility is that the thermally induced switching of distinct intrashell domains may be correlated, possibly involving a stochastic process within this temperature range. Further studies are in progress to better understand this complex behavior. We also note that repeated cycling of the magnetic hysteresis at 5 K will gradually decrease H_E by the so-called training effect.[12,20,37] This is consistent with the notion that the frozen interfacial spins can relax into random orientations after multiple cycles of magnetic field with subsequent loss of EB.

IV. CONCLUSION

In summary, we present evidence that frozen interfacial spins play a key role in mediating exchange bias and enhancing coercivity in composite nanoparticles, based on a comparative analysis of Fe/Fe_3O_4 core-shell nanoparticles and Fe_3O_4 hollow-shell nanoparticles. The frozen interfacial spins comprise only a small fraction of the total magnetic moment, yet can mediate a strong exchange coupling between the core and shell domains under field-cooled conditions. Magnetization studies performed with uniform, well-dispersed particles also enabled us to identify an abrupt demagnetization of shell moments at low field, one which is strongly influenced by the degree of alignment of the interfacial spins. These studies further illustrate the breadth and significance of exchange bias in nanoscale magnetism.

ACKNOWLEDGMENTS

This work is supported by the U.S. Department of Energy (DOE), BES-Materials Sciences, under Contract No. DE-AC02-06CH11357, by DOE Center for Nanoscale Materials, and by the National Science Foundation. X.M.L. thanks M. Bode for fruitful discussions.

[1] W. H. Meiklejohn and C. P. Bean, Phys. Rev. **102**, 1413 (1956).
[2] A. E. Berkowitz and K. Takano, J. Magn. Magn. Mater. **200**, 552 (1999).
[3] J. Nogués, J. Sort, V. Langlais, V. Skumryev, S. Suriñach, J. S. Muñoz, and M. D. Baró, Phys. Rep. **422**, 65 (2005).
[4] U. Nowak, K. D. Usadel, J. Keller, P. Miltényi, B. Beschoten, and G. Güntherodt, Phys. Rev. B **66**, 014430 (2002).
[5] D. Suess, M. Kirschner, T. Schrefl, J. Fidler, R. L. Stamps, and J.-V. Kim, Phys. Rev. B **67**, 054419 (2003).
[6] A. P. Malozemoff, J. Appl. Phys. **63**, 3874 (1988).
[7] W. Kuch, L. I. Chelaru, F. Offi, J. Wang, M. Kotsugi, and J. Kirschner, Nature Mater. **5**, 128 (2006).
[8] P. J. van der Zaag, R. M. Wolf, A. R. Ball, C. Bordel, L. F. Feiner, and R. Jungblut, J. Magn. Magn. Mater. **148**, 346 (1995).
[9] M. Ali, P. Adie, C. H. Marrows, D. Greig, B. J. Hickey, and R. L. Stamps, Nature Mater. **6**, 70 (2007).
[10] R. H. Kodama, A. E. Berkowitz, E. J. McNiff, Jr., and S. Foner, Phys. Rev. Lett. **77**, 394 (1996).
[11] B. Martínez, X. Obradors, L. I. Balcells, A. Rouanet, and C. Monty, Phys. Rev. Lett. **80**, 181 (1998).
[12] R. K. Zheng, G. H. Wen, K. K. Fung, and X. X. Zhang, J. Appl. Phys. **95**, 5244 (2004).
[13] T. Hyeon, Chem. Commun. (Cambridge) **2003**, 927.
[14] S. Peng, C. Wang, J. Xie, and S. Sun, J. Am. Chem. Soc. **128**, 10676 (2006).
[15] V. Skumryev, S. Stoyanov, Y. Zhang, G. Hadjipanayis, D. Givord, and J. Nogués, Nature (London) **423**, 850 (2003).
[16] J. B. Tracy, D. N. Weiss, D. P. Dinega, and M. G. Bawendi, Phys. Rev. B **72**, 064404 (2005).
[17] S. E. Inderhees, J. A. Borchers, K. S. Green, M. S. Kim, K. Sun, G. L. Strycker, and M. C. Aronson, Phys. Rev. Lett. **101**, 117202 (2008).
[18] D. W. Kavich, J. H. Dickerson, S. V. Mahajan, S. A. Hasan, and J.-H. Park, Phys. Rev. B **78**, 174414 (2008).
[19] H. Zeng, S. Sun, J. Li, Z. L. Wang, and J. P. Liu, Appl. Phys. Lett. **85**, 792 (2004).
[20] C. Martínez-Boubeta, K. Simeonidis, M. Angelakeris, N. Pazos-Pérez, M. Giersig, A. Delimitis, L. Nalbandian, V. Alexandrakis, and D. Niarchos, Phys. Rev. B **74**, 054430 (2006).
[21] M. Vasilakaki and K. N. Trohidou, Phys. Rev. B **79**, 144402 (2009).
[22] P. J. van der Zaag, Y. Ijiri, J. A. Borchers, L. F. Feiner, R. M. Wolf, J. M. Gaines, R. W. Erwin, and M. A. Verheijen, Phys. Rev. Lett. **84**, 6102 (2000).
[23] H. Ohldag, A. Scholl, F. Nolting, E. Arenholz, S. Maat, A. T. Young, M. Carey, and J. Stöhr, Phys. Rev. Lett. **91**, 017203 (2003).
[24] M. Gruyters, Phys. Rev. Lett. **95**, 077204 (2005).
[25] D. L. Peng, T. Hihara, K. Sumiyama, and H. Morikawa, J. Appl. Phys. **92**, 3075 (2002).
[26] L. Del Bianco, D. Fiorani, A. M. Testa, E. Bonetti, and L. Signorini, Phys. Rev. B **70**, 052401 (2004).
[27] C. Baker, S. K. Hasanain, and S. I. Shah, J. Appl. Phys. **96**, 6657 (2004).
[28] F. C. Voogt, T. Fujii, T. Hibma, M. Hoefman, P. J. M. Smulders, G. H. Wijnja, G. L. Zhang, and L. Niesen, Hyperfine Interact. **97-98**, 99 (1996).

[29] R. Jungblut, R. Coehoorn, and M. T. Johnson, J. aan de Stegge, and A. Reinders, J. Appl. Phys. **75**, 6659 (1994).
[30] A. B. van Groenou, P. F. Bongers, and A. L. Stuyts, Mater. Sci. Eng. **3**, 317 (1969).
[31] D. V. Dimitrov, A. S. Murthy, G. C. Hadjipanayis, and C. P. Swann, J. Appl. Phys. **79**, 5106 (1996).
[32] J. Nogués and I. K. Schuller, J. Magn. Magn. Mater. **192**, 203 (1999).
[33] E. Lima, Jr., A. L. Brandl, A. D. Arelaro, and G. F. Goya, J. Appl. Phys. **99**, 083908 (2006).
[34] C. Leighton, M. R. Fitzsimmons, P. Yashar, A. Hoffmann, J. Nogués, J. Dura, C. F. Majkrzak, and I. K. Schuller, Phys. Rev. Lett. **86**, 4394 (2001).
[35] P. V. Hendriksen, J. Phys.: Condens. Matter **5**, 5675 (1993).
[36] Data in panel (b) was collected on the same sample as panel (a) after exposure to air for three months. The slight change in H_E and H_C values at 5 K is due to the aging of the sample and will be discussed in a future publication.
[37] C. Schlenker, S. S. P. Parkin, J. C. Scott, and K. Howard, J. Magn. Magn. Mater. **54-57**, 801 (1986).